Bursting oscillations in a hydro-turbine governing system with two time scales*

Qing-Shuang Han(韩青爽)[1], Di-Yi Chen(陈帝伊)[1,2,†], and Hao Zhang(张浩)[1]

[1] *Institute of Water Resources and Hydropower Research, Northwest A & F University, Yangling* 712100, *China*
[2] *Key Laboratory of Agricultural Soil and Water Engineering in Arid and Semiarid Areas, Ministry of Education, Northwest A & F University, Yangling* 712100, *China*

(Received 14 May 2017; revised manuscript received 5 August 2017; published online 20 October 2017)

A fast-slow coupled model of the hydro-turbine governing system (HTGS) is established by introducing frequency disturbance in this paper. Based on the proposed model, the performances of two time scales for bursting oscillations in the HTGS are investigated and the effect of periodic excitation of frequency disturbance is analyzed by using the bifurcation diagrams, time waveforms and phase portraits. We find that stability and operational characteristics of the HTGS change with the value of system parameter k_d. Furthermore, the comparative analyses for the effect of the bursting oscillations on the system with different amplitudes of the periodic excitation a are carried out. Meanwhile, we obtain that the relative deviation of the mechanical torque m_t rises with the increase of a. These methods and results of the study, combined with the performance of two time scales and the fast-slow coupled engineering model, provide some theoretical bases for investigating interesting physical phenomena of the engineering system.

Keywords: bursting oscillations, physical phenomena, hydro-turbine governing system, two time scales

PACS: 82.40.Bj, 88.60.K–, 88.40.fc, 02.30.Hq **DOI:** 10.1088/1674-1056/26/12/128202

1. Introduction

The multi time-scale phenomenon which results from the actual time effect, spatial effect, structural effect and physical effect in a real system, exists in many complex mathematical models.[1–3] The complex mathematical model in which the state variables have very different changing rates is called the fast-slow coupled model.[4–8] The response of a fast-slow coupled system is performed by the alternate change of large amplitude oscillation (i.e, spiking state) and micro amplitude oscillation (i.e, quiescent state). The time history and the trajectory connecting the two special behavior process are referred to as bursting oscillations.[9–11]

Multi time-scale dynamics can reveal nonlinear essential characteristics of the system from the dynamic point of view, and it is extensively used in biology, chemistry, life sciences, physics, etc.[12–17] For example, Gu *et al.*[18] not only revealed the nonlinear dynamics of the firing patterns of neural pacemakers but also provided experimental evidence for the existence of bifurcations from bursting to spiking simulated by using the theoretical models. Song and Xu[19] showed that the time delay must be large enough for bursting behavior to occur in a delayed system and the different bursting behaviors are related to the delay coupling and external inputs. Ji and Bi[20] found that the multiple crossing bifurcation, which is the combination of the Hopf bifurcation and the turning point bifurcation and occurs at the non-smooth boundaries, causes the periodic buster to the quasi-periodic oscillation. Guo *et al.*[21] investigated how intrinsic channel noise affects the response of stochastic Hodgkin–Huxley neuron to external fluctuating inputs with different amplitudes and correlation times. Hou *et al.*[22] investigated the fractional-order Belousov–Zhabotinsky (BZ) reaction with different time scales and studied the slow-fast effect in fractional-order BZ reaction with two time scales coupled.

As is well known, few researchers concentrate on modeling and analyzing the fast-slow coupled engineering system such as the HTGS. The HTGS is a complex nonlinear, time-variant and non-minimum phase system involving hydro dynamics, mechanical dynamics, and electrical dynamics. From the point of view of dynamically coupled hydraulic-mechanical-electric-structural system for a hydropower station, the parameters in the HTGS can be divided into a fast transmission rate (electrical transient) and slow strain rate (hydraulic transient).[23,24] In recent years, achievements about modeling and controlling of the HTGS are becoming more and more abundant. For example, Zhang *et al.*[25] and Li *et al.*[26–28] concentrated on the modeling and analyzing of

*Project supported by the Scientific Research Foundation of the National Natural Science Foundation of China–Outstanding Youth Foundation (Grant No. 51622906), the National Natural Science Foundation of China (Grant No. 51479173), the Fundamental Research Funds for the Central Universities, China (Grant No. 201304030577), the Scientific Research Funds of Northwest A & F University, China (Grant No. 2013BSJJ095), the Science Fund for Excellent Young Scholars from Northwest A & F University (Grant No. Z109021515), and the Shaanxi Provincial Nova Program, China (Grant No. 2016KJXX-55).

†Corresponding author. E-mail: diyichen@nwsuaf.edu.cn

© 2017 Chinese Physical Society and IOP Publishing Ltd

the HTGS in the process of large fluctuation. Zeng *et al.*[29] and Xu *et al.*[30] focused on Hamiltonian mathematical modeling of HTGS which can be used to describe general open systems with the structure of energy dissipation and the exchange of energy with the environment. Pico *et al.*[31] presented an investigation of hydro power plants with pelton-type turbine-generator sets and robust control theory was used to design a hydro-stabilizer. Salhi *et al.*[32] stated an approach to modeling and controlling a micro hydro power plant considered as a non-linear system by using a Takagi–Sugeno fuzzy system. Husek[33] presented a proportional-integral-derivative controller design for hydraulic turbine based on sensitivity margin specifications. These research results not only explain many complex phenomena in the actual operation of the hydropower station, but also provide a theoretical basis for the safe and stable operation of the hydropower station system. Although great achievements have been made in autonomous HTGS with single time scale, many time-relative non-autonomous factors existing in the real HTGS with multi time-scale have not been considered carefully. Some complex disturbances that are defined as risks constantly occur in the process of operation of the HTGS, like the load disturbance, the frequency disturbance, and the flow rates disturbance.[34] Besides, the non-autonomous factors not only change the structure of the HTGS, but also make the system more complex. Therefore, it is necessary to study the non-autonomous HTGS with multi time-scale, which will provide a theoretical basis for studying the operation stability and control strategy for the system.

In this paper, a mathematical model of the non-autonomous HTGS with two time scales is proposed by introducing frequency disturbance as periodic excitation. Next, compared with the traditional model of HTGS, the stabilities and dynamic behaviors of the mathematic model of non-autonomous HTGS with two time scales are investigated by numerical simulation. Besides, combining the time waveforms and the phase portraits, the phenomena of the bursting oscillations are described in detail. At the same time, the bursting oscillations of the system, with different amplitudes of periodic excitation, are analyzed by numerical simulation. Finally, the conclusions of this study and discussion about future work are presented.

The rest of the paper is organized as follows. In Section 2, a mathematical model of the non-autonomous HTGS with two time scales is established. In Section 3 its dynamic behaviors are analyzed and described are the phenomena of the bursting oscillations in the above model. In Section 4, some conclusions are drawn from this study.

2. Modeling of the non-autonomous HTGS with two time scales

As shown in Fig. 1,[35] the HTGS consists of four parts, i.e., a hydro-turbine, a hydraulic system, a generator and a controller. In view of that the four parts of the HTGS were discussed in the previous papers,[23–28] and here we will directly utilize the four parts. Therefore, based on the four parts, in this section we directly give the traditional mathematical model of the autonomous HTGS with a single time scale. Then, a mathematical model of the non-autonomous HTGS with two time scales is established by introducing the periodic excitation.

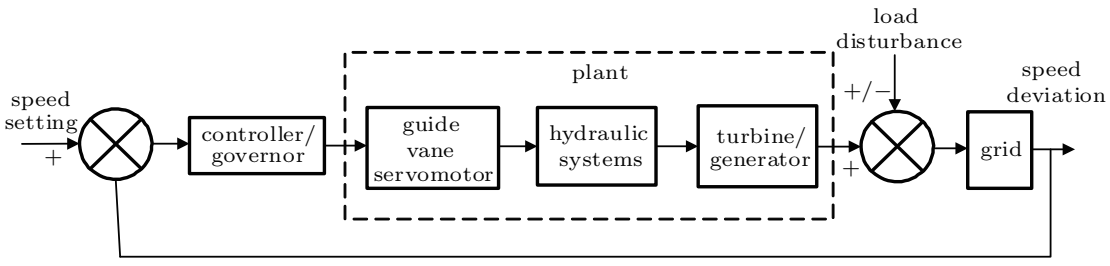


Fig. 1. Diagrammatic sketch of the HTGS.

2.1. Traditional mathematical model of the autonomous HTGS with single time scale

The dynamic characteristics of generator and load can be described by[23,36]

$$T_{ab}\frac{\mathrm{d}x}{\mathrm{d}t}+e_n x = m_{\mathrm{t}} - m_{g0}, \tag{1}$$

where T_{ab} is the mechanical starting time, e_n is the synthetic self-regulation coefficient, x is the deviation of the hydro-turbine speed, m_{t} is the deviation of the mechanical torque of the hydro-turbine, and m_{g0} is the load torque disturbance.

The dynamic model of the hydro-turbine and hydraulic systems can be expressed as[37]

$$m_{\mathrm{t}} = e_y y - e_y e T_w \frac{\mathrm{d}y}{\mathrm{d}t} - e_{qx} e_h T_w \frac{\mathrm{d}x}{\mathrm{d}t} - e_{qh} T_w \frac{\mathrm{d}m_{\mathrm{t}}}{\mathrm{d}t}, \tag{2}$$

where y, e_y, e, T_w, e_{qx}, e_h, and e_{qh} respectively denote the deviation of the guide vane opening, partial derivatives of the

mechanical torque with respect to the guide vane opening, the intermediate variable, the water starting time, partial derivatives of the flow with respect to the speed, the mechanical torque with respect to the head of the hydro-turbine, and partial derivatives of the flow with respect to the head of the hydro-turbine.

The speed governor is composed of a controller and a guide vane servomotor. The output signal of the PID controller can be written as[25,27]

$$u = k_{\mathrm{p}}(r-x) + k_{\mathrm{i}} z - k_{\mathrm{d}}\dot{x}, \tag{3}$$

where u, k_{p}, r, k_{i}, z, and k_{d} respectively represent the output of the regulator, the proportional adjustment coefficient, the reference input of the generator speed, the integral adjustment coefficient, the intermediate variable, and the differential adjustment coefficient.

The dynamic characteristics of a guide vane servomotor[28] can be described as

$$T_y \frac{\mathrm{d}y}{\mathrm{d}t} + y = u, \tag{4}$$

where T_y is the engager relay time constant.

Based on the modular modeling method,[24–28,36] a traditional mathematical model of the autonomous HTGS with single time scale can be described as follows:

$$\begin{cases} \dot{x} = \dfrac{m_{\mathrm{t}}}{T_{ab}} - \dfrac{m_{g0}}{T_{ab}} - e_n x, \\ \dot{y} = \dfrac{1}{T_y}\left[k_{\mathrm{p}}(r-x) + k_{\mathrm{i}} z - k_{\mathrm{d}}\left(\dfrac{m_{\mathrm{t}}}{T_{ab}} - \dfrac{m_{g0}}{T_{ab}} - e_n x\right) - y\right], \\ \dot{z} = r - x, \\ \dot{m}_{\mathrm{t}} = \dfrac{1}{e_{qh}T_w}\left\{ -m_{\mathrm{t}} + e_{my} y - \dfrac{e_{my} e T_w}{T_y} \right. \\ \qquad \times \left[k_{\mathrm{p}}(r-x) + k_{\mathrm{i}} z - k_{\mathrm{d}}\left(\dfrac{m_{\mathrm{t}}}{T_{ab}} - \dfrac{m_{g0}}{T_{ab}} - e_n x\right) - y\right] \\ \qquad \left. - e_{qx} e_{mh} T_w \left(\dfrac{m_{\mathrm{t}}}{T_{ab}} - \dfrac{m_{g0}}{T_{ab}} - e_n x\right)\right\}. \end{cases} \tag{5}$$

2.2. Mathematical model of the HTGS with periodic excitation

There are many time-relative non-autonomous factors in the real HTGS, such as the frequency disturbance in the operation process of the hydropower station. Generally, the frequency disturbance in the system is caused by the fluctuation of grid load with the change of time.[37,38] Here, we consider the frequency disturbance of the HTGS as a periodic excitation. We set this periodic excitation as x_s, and $x_s = a\sin\omega t$, where a and ω are respectively the amplitude and the frequency of the periodic excitation. Thus, a mathematical model of the HTGS with the periodic excitation is obtained as

$$\begin{cases} \dot{x} = \dfrac{m_{\mathrm{t}}}{T_{ab}} - \dfrac{m_{g0}}{T_{ab}} - \dfrac{e_n(x + a\sin\omega t)}{T_{ab}}, \\ \dot{y} = \dfrac{1}{T_y}\left[k_{\mathrm{p}}(r - (x + a\sin\omega t)) + k_{\mathrm{i}} z \right. \\ \qquad \left. - k_{\mathrm{d}}\left(\dfrac{m_{\mathrm{t}}}{T_{ab}} - \dfrac{m_{g0}}{T_{ab}} - e_n(x + a\sin\omega t)\right) - y\right], \\ \dot{z} = r - (x + a\sin\omega t), \\ \dot{m}_{\mathrm{t}} = -\dfrac{e_y e T_w}{T_y}\dfrac{1}{e_{qh}T_w}\left[k_{\mathrm{p}}(r - x - a\sin\omega t) + k_{\mathrm{i}} z \right. \\ \qquad \left. - k_{\mathrm{d}}\left(\dfrac{m_{\mathrm{t}}}{T_{ab}} - \dfrac{m_{g0}}{T_{ab}} - e_n(x + a\sin\omega t)\right) - y\right] \\ \qquad - e_{qx} e_h T_w \dfrac{1}{e_{qh}T_w}\left(\dfrac{m_{\mathrm{t}}}{T_{ab}} - \dfrac{m_{g0}}{T_{ab}} - e_n(x + a\sin\omega t)\right) \\ \qquad - \dfrac{1}{e_{qh}T_w} m_{\mathrm{t}} + \dfrac{1}{e_{qh}T_w} e_y y. \end{cases} \tag{6}$$

In this paper, the value of the periodic excitation frequency ω is selected as 10^4, which can be treated as a parameter of fast transmission rate. That is to say, the frequency of the periodic excitation is far greater than that in the traditional system. Thus, a model of the non-autonomous HTGS with two time scales is established by selecting an appropriate value of periodic excitation frequency.

3. Physical phenomena of bursting oscillations

In this section, a traditional model and a fast–slow coupled model of the HTGS are used to study the dynamical characteristics of the HTGS with two time scales. Here, the numerical simulations are carried out by using the Runge–Kutta method. Specifically, the initial values of [$\dot{x}$, $\dot{y}$, $\dot{z}$, $\dot{m}_{\mathrm{t}}$] in Eqs. (5) and (6) are [0.001, 0.001, 0.001, 0.001,] and the iteration step is 2000 for each simulation. The values of HTGS parameters are shown in Table 1.

Table 1. Values of HTGS parameters.

Parameters	Values	Units	Parameters	Values	Units
e_{qh}	0.50	p.u.	T_w	2.00	s
e_{qx}	0.01	p.u.	T_y	1.00	s
e_{qy}	1.00	p.u.	r	0.001	s
e_{mh}	1.50	p.u.	m_{g0}	0.001	s
e_{my}	1.00	p.u.	k_{p}	2.00	p.u.
e	1.00	p.u.	k_{i}	1.00	s^{-1}
e_n	1.00	s	a	0.001	s
T_{ab}	8.00	s			

Bifurcation diagrams of the mechanical torque m_{t} with respect to the governor parameter k_{d} are presented in Fig. 2 to study the stability and operational feature of the HTGS. Then, the bifurcation diagram and its local amplification of a traditional model of the HTGS are obtained as shown in Figs. 2(a) and 2(b), respectively. The bifurcation diagrams of the mechanical torque m_{t} with respect to the governor parameter k_{d} are also presented in Figs. 2(c) and 2(d).

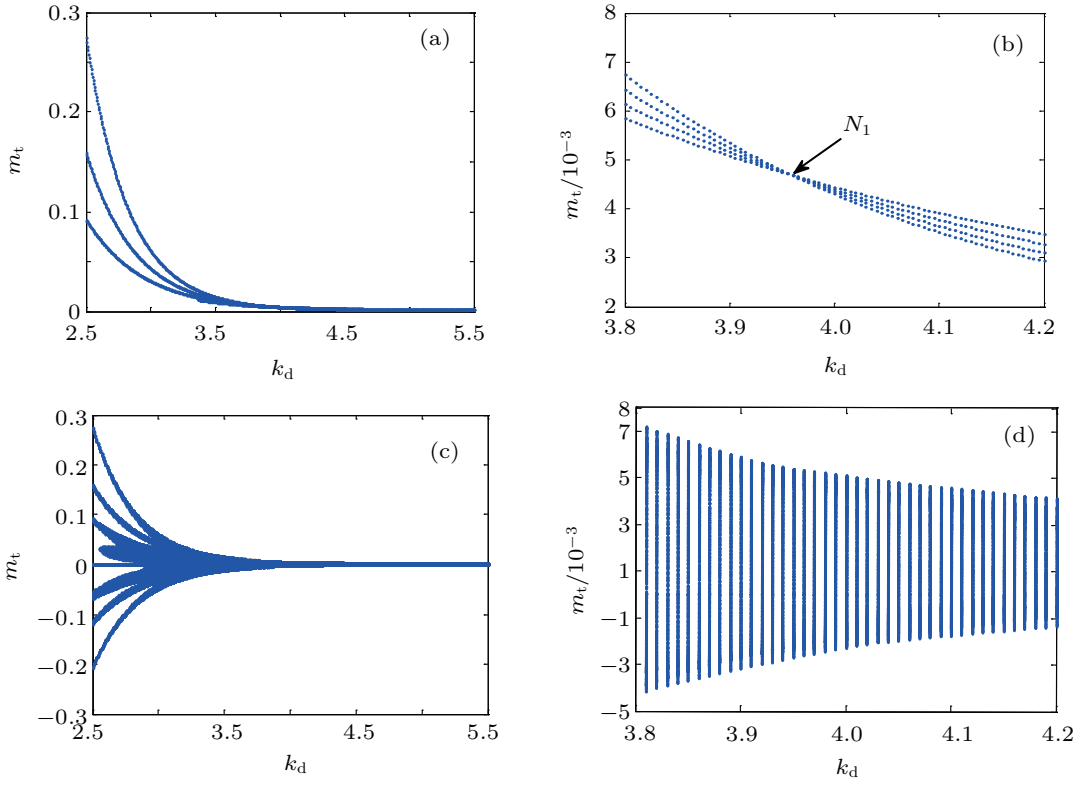


Fig. 2. (color online) Bifurcation diagrams of the mechanical torque m_t with respect to the governor parameter k_d: (a) bifurcation diagram of the autonomous HTGS with single time scale at $2.5 \leq k_d \leq 5.5$; (b) local amplification of the bifurcation diagram of the autonomous HTGS with single time scale at $3.8 \leq k_d \leq 4.2$; (c) bifurcation diagram of the non-autonomous HTGS with two time scales at $2.5 \leq k_d \leq 5.5$; and (d) local amplification of the bifurcation diagram of the non-autonomous HTGS with two time scales at $3.8 \leq k_d \leq 4.2$.

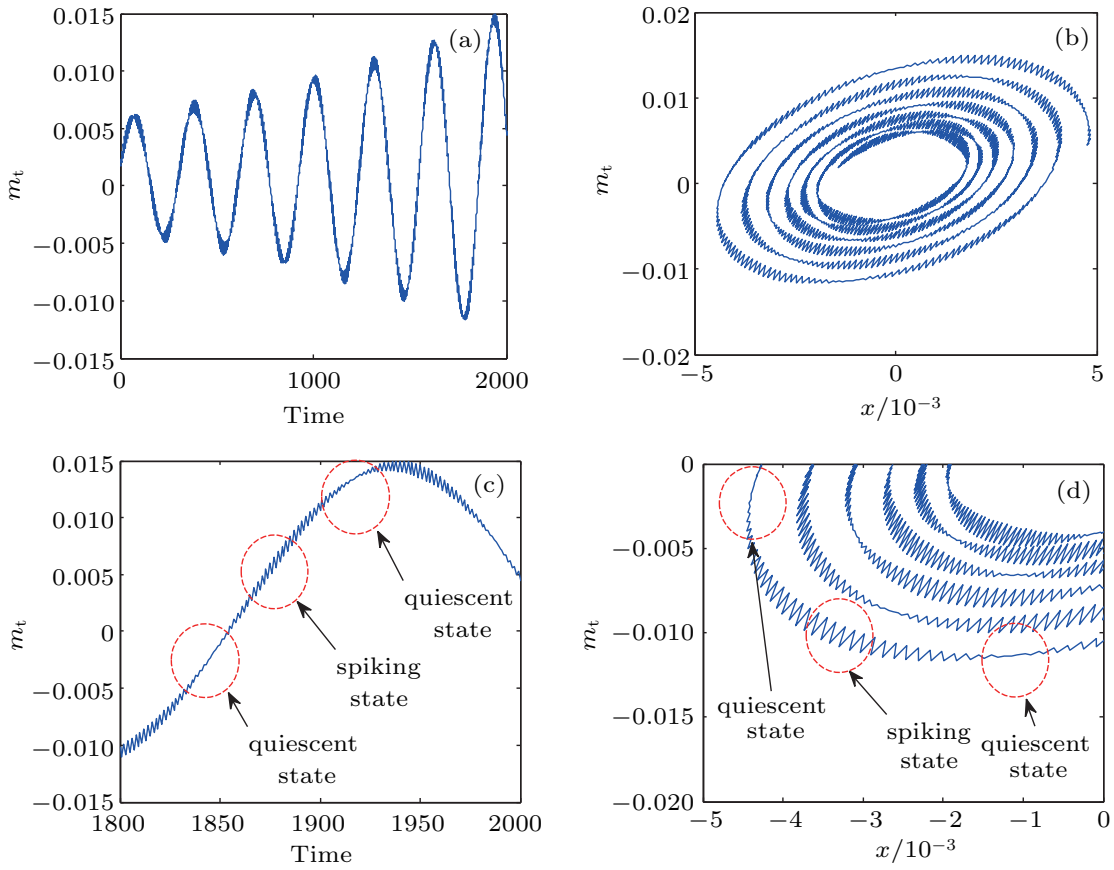


Fig. 3. (color online) Time waveform and phase orbit of the non-autonomous HTGS with two time scales at $k_d = 3.5$. (a) Time waveform with m_t–t, (b) phase orbit with m_t–x, (c) local amplification of the time waveform with 1800 < time < 2000, and (d) local amplification of the phase orbit with m_t–x.

From Figs. 2(a)–2(b), when $2.5 \leq k_d \leq 3.96$, the maximum of the relative deviation of the mechanical torque m_t decreases gradually and the track becomes narrow with the increase of k_d. For $3.96 \leq k_d \leq 5,5$, the maximum of m_t first decreases and then gradually tends to be zero with increasing k_d, which indicates that the governing system operates in a steady state. Note that there is an important bifurcation point, namely $k_d = 3.96$, which is consistent with N_1 in Fig. 2(b). At this point, the system is in a critical state.

Figures 2(c)–2(d) show bifurcation diagrams of a fast-slow coupled model of the HTGS with two time scales. Meanwhile, figures 2(c)–2(d) show more interesting physical phenomena than the bifurcation diagrams of a traditional model of the HTGS. Firstly, the relative deviation of the mechanical torque m_t includes negative values. In addition, the maximum of m_t increases by more than five percent when $m_d = 2.5$. For $2.5 \leq k_d \leq 3$, the values of m_t show a fan-shaped trend and then gradually tends to be zero with increasing k_d. Comparison of Fig. 2(d) with Fig. 2(b) which have typical Hopf bifurcation lines and critical point, shows that figure 2(b) has no obvious critical point and the value of m_t fluctuating between -0.004 and 0.007. Furthermore, the maximum of m_t is less than 0.007 when $k_d = 3.8$ in Fig. 2(b), but the maximum of m_t is obviously bigger than 0.007 in Fig. 2(d). All of these results show that the frequency disturbance introduced into the traditional model of the HTGS makes the physical phenomena more complex.

In order to further study the dynamical behaviors of the system with two time scales, we select three typical points in Fig. 2(c), which are $k_d = 3.5$, $k_d = 3.96$, and $k_d = 4.5$. Time waveforms and phase orbits are presented as shown below.

For $k_d = 3.5$, as shown in Fig. 3(a), the relative deviation of the mechanical torque m_t appears as periodically increasing oscillation as time goes on. The periodic boundary points emerge clearly in the wave crest and trough at the first half of the time, and they seem to disappear at the last part of the time. The phase orbit with m_t–x described in Fig. 3(b) is divergent gradually and the thickness of track line changes back and forth alternately. The corresponding magnifications shown in Figs. 3(c) and 3(d) are utilized to further analyze the dynamic behavior of the system with two time scales. As shown in Fig. 3(c), the track line of m_t has the characteristic of a periodic oscillation between the micro amplitude oscillation and the stationary state, which indicates that the spiking state and the quiescent state are alternately periodic. From Fig. 3(d), it is clear that there are transitions between the spiking state and the quiescent state in the system. These results indicate that the HTGS exhibits a bursting oscillation phenomenon over time and is in an unstable state.

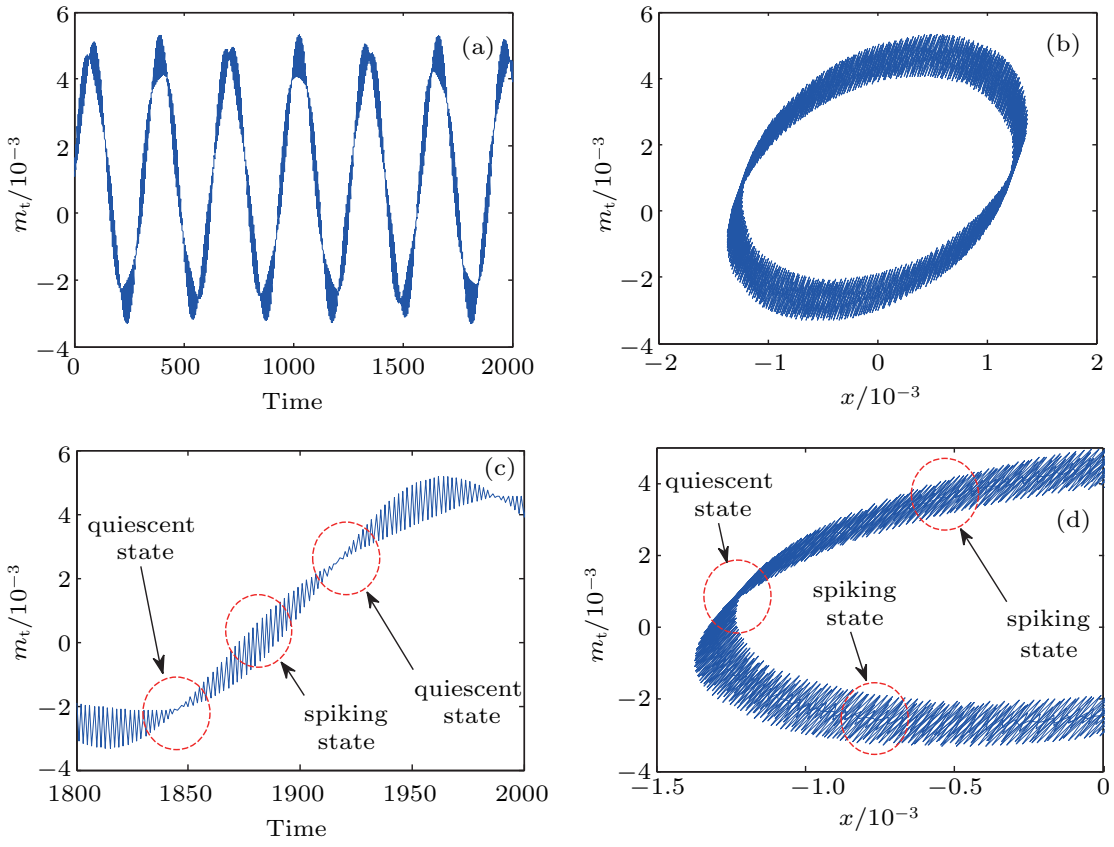


Fig. 4. (color online) Time waveform and phase orbit of the non-autonomous HTGS with two time scales at $k_d = 3.96$. (a) Time waveform with m_t–t, (b) phase orbit with m_t–x, (c) local amplification of the time waveform with 1800 < time < 2000, and (d) local amplification of the phase orbit with m_t–x.

Figure 4(a) shows a time waveform of m_t with $k_d = 3.96$. The amplitude of m_t does not change as time varies. In addition, a more obvious oscillation phenomenon and a clear demarcation point occur near the wave crest and trough. Figure 4(b) shows phase orbit with $k_d = 3.96$, which has two distinct intersections near $m_t = 0$. The dynamic law of the interaction between the spiking state and the quiescent state of the system is clearly shown in Figs. 4(c) and 4(d). Therefore, the HTGS turns a periodic vibration into a bursting oscillation.

The responses of the HTGS with $k_d = 4.5$ are shown in Fig. 5. From Fig. 5(a), it is obviously observed that m_t presents a periodic decay oscillation and has the similar characteristics to those in Figs. 3(a) and 4(a) near the wave crest and trough. It can be seen that the trajectory of m_t changes significantly at the second half of the time, which indicates that the effect of periodic oscillation on system behavior is becoming more and more serious as time goes by. As shown in Fig. 5(b), the track line of the system converts between the sharp shock and micro shock, which presents a chaotic state. The states of the spiking and the quiescent are described in detail in Figs. 5(c) and 5(d). These results illustrate that the system keeps steady at $k_d = 4.5$ and the bursting oscillation has a great influence on the stability of the system.

In order to reveal the bursting oscillation of the system with the amplitude of the periodic excitation, time waveforms and phase orbits are presented with different values of the amplitude of the periodic excitation a at $k_d = 3.96$, namely $a = 0.00$, $a = 0.001$, $a = 0.005$, and $a = 0.01$.

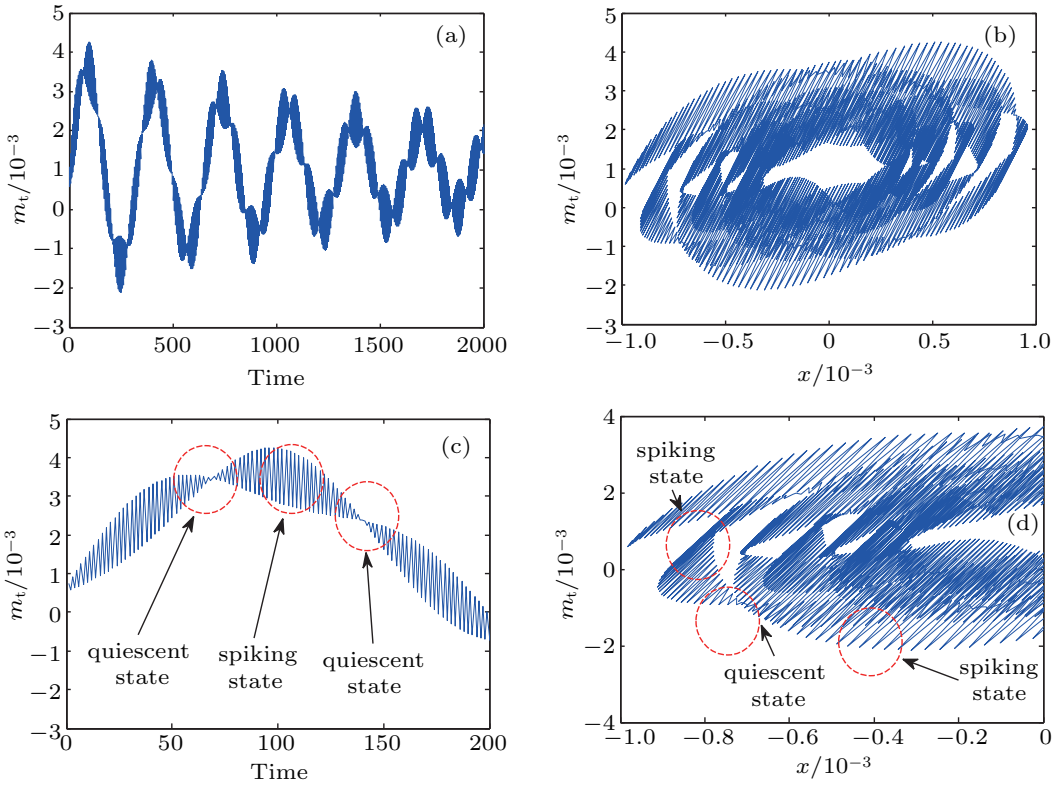


Fig. 5. (color online) Time waveform and phase orbit of the non-autonomous HTGS with two time scales at $k_d = 4.5$. (a) Time waveform with m_t–t, (b) phase orbit with m_t–x, (c) local amplification of the time waveform with $0 <$ time < 200, and (d) local amplification of the phase orbit with m_t–x.

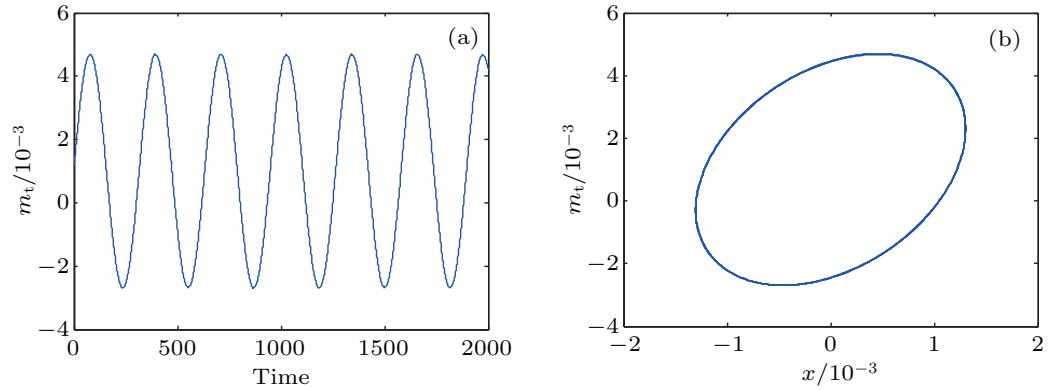


Fig. 6. (color online) Time waveform and phase orbit of the autonomous HTGS with single time scale for $a = 0.00$ at $k_d = 3.96$. (a) Time waveform with m_t–t, (b) local amplification of the time waveform with $1800 <$ time < 2000.

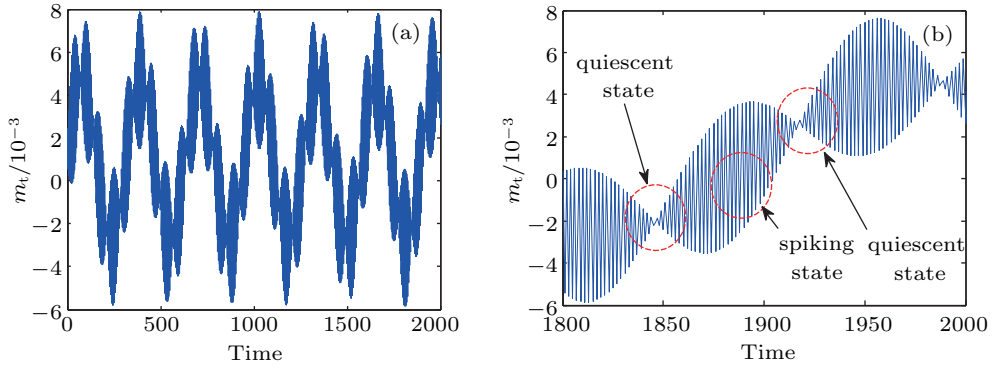


Fig. 7. (color online) Time waveform and phase orbit of the non-autonomous HTGS with two time scales for $a = 0.005$ at $k_d = 3.96$. (a) Time waveform with m_t–t, and (b) local amplification of the time waveform with 1800 < time < 2000.

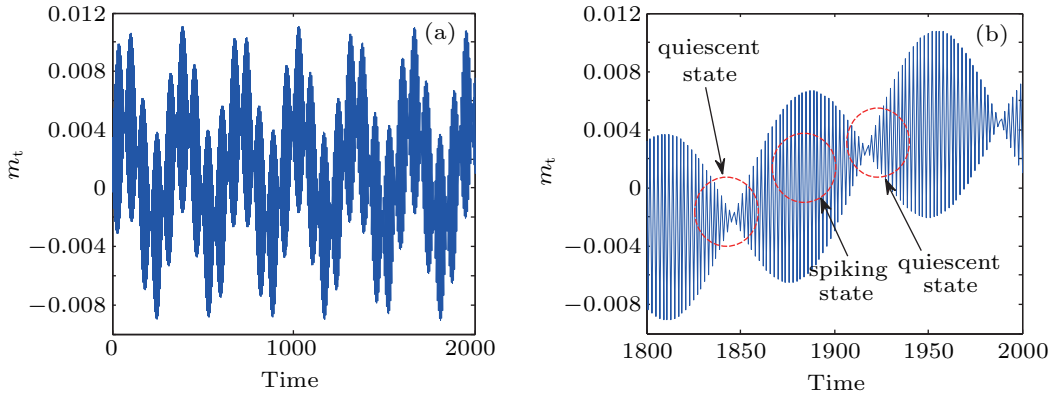


Fig. 8. (color online) Time waveform and phase orbit of the non-autonomous HTGS with two time scales for $a = 0.01$ at $k_d = 3.96$. (a) Time waveform with m_t–t, (b) local amplification of the time waveform with 1800 < time < 2000.

The value of the amplitude of the periodic excitation is equal to 0.00, which means that the frequency disturbance does not occur in the operation process of the hydropower station. For $a = 0.00$, as shown in Fig. 6, the motion regularity of the hydro-turbine mechanical torque m_t is periodical and a limit cycle appears in the phase orbit. Besides, the maximal value of m_t is approximately equal to 4.5×10^{-3}. The results indicate that the governing system is in a critical state. For $a = 0.001$ and $k_d = 3.95$, as shown in Fig. 4, the bursting oscillations of the system behave as that described above and the maximal value of m_t is nearly equal to 5.0×10^{-3}. Figure 7 shows the time waveform and local amplification of the time waveform with $a = 0.005$. It can be seen that the phenomenon is almost the same as that in Fig. 4, while the maximal value of m_t is about 8.0×10^{-3}. As shown in Fig. 8, the hydro-turbine mechanical torque m_t with $a = 0.01$ tends to be more complex due to the stronger bursting oscillations effect. The maximal value of the relative deviation of the mechanical torque m_t is bigger than those in Figs. 4–6, which means that vibration of the system in this case is more intense.

These results show that the amplitude of the periodic excitation has a great influence on the dynamic behaviors of the system. As the value of the amplitude of the periodic excitation a increases, the effect of the bursting oscillations on the system becomes stronger.

4. Conclusions and discussion

The HTGS is a complex nonlinear, time-varying, and non-minimum phase system involving hydro dynamics, mechanical dynamics, and electrical dynamics, which is accurately a multi-time-scale dynamic system. However, few papers have reported on the fast–slow dynamical analysis of a typical complex engineering system coupled hydraulic-mechanical-electric-structure.

In this paper, some interesting physical phenomena of the non-autonomous HTGS with two time scales are investigated. First, the stabilities and dynamic behaviors of the above system are investigated in detail by numerical simulation, which is carried out by using the Runge–Kutta method. Meanwhile, the bifurcation diagram of a traditional model of the HTGS is presented to further study the bifurcation characteristics for the system with two time scales. Third, three typical points are respectively selected based on the bifurcation diagram. Then, the physical phenomena of the bursting oscillations existing in the system with two time scales are described in detail with the combination of the time waveforms and the phase portraits. From an experimental point of view, the spiking state and the quiescent state alternate periodically as the time goes

by. Also, stability and operational characteristics vary with system parameter k_d. Finally, the comparative analyses for the effect of the bursting oscillations on the system with different amplitudes of the periodic excitation a are carried out. We obtain that the relative deviation of the mechanical torque m_t rises with the increase of a.

The future work will involve the investigation into the bifurcation characteristics in theory of the non-autonomous HTGS with two time scales. In addition, the numerical experiments will focus far more on the behavior characteristics of the HTGS with two time scales in the transient process.

References

[1] Desroches M, Guckenheimer J, Krauskopf B, Kuehn C, Osinga H M and Wechselberger M 2012 *SIAM Rev.* **54** 211
[2] Han X J, Bi Q S, Ji P and Kurths J 2015 *Phys. Rev. E* **92** 012911
[3] Pal V, Tradonsky C, Chriki R, Friesem A A and Davidson N 2017 *Phys. Rev. Lett.* **119** 013902
[4] Fallah H 2016 *Int. J. Bifur. Chaos* **26** 1630022
[5] Desroches M, Guillamon A, Ponce E, Prohens R, Rodrigues S and Teruel A E 2016 *SIAM Rev.* **58** 653
[6] Wu T Y, Chen X K, Zhang Z D, Zhang X F and Bi Q S 2017 *Acta Phys. Sin.* **66** 110501 (in Chinese)
[7] Ding X L and Li Y Y 2016 *Acta Phys. Sin.* **65** 210502 (in Chinese)
[8] Shen M and Zhao L 2014 *Chin. Phys. Lett.* **31** 010401
[9] Zhang Z D, Liu Y, Zhang S Z and Bi Q S 2017 *Acta Phys. Sin.* **66** 020501 (in Chinese)
[10] Sevilla-Escoboza R, Buldu J M, Pisarchik A N, Boccaletti S and Gutierrez R 2015 *Phys. Rev. E* **91** 032902
[11] Nesse W H, Del Negro C A and Bressloff P C 2008 *Phys. Rev. Lett.* **101** 088101
[12] Yanchuk S and Giacomelli G 2015 *Phys. Rev. E* **92** 042903
[13] Biferale L, Bonaccorso F, Mazzitelli I M, van Hinsberg M A T, Lanotte A S, Musacchio S, Perlekar P and Toschi F 2016 *Phys. Rev. X* **6** 041036
[14] Li X H and Bi Q S 2012 *Chin. Phys. B* **21** 060505
[15] Zhang Y and Bi Q S 2011 *Chin. Phys. B* **20** 010504
[16] Wang H X, Wang Q Y and Lu Q S 2011 *Chaos, Solitons and Fractals* **44** 667
[17] Zhang X F, Wu L and Bi Q S 2016 *Chin. Phys. B* **25** 070501
[18] Gu H G, Pan B B, Chen G R and Duan L X 2014 *Nonlinear Dyn.* **78** 391
[19] Song Z G and Xu J 2012 *Nonlinear Dyn.* **67** 309
[20] Ji Y and Bi Q S 2010 *Phys. Lett. A* **374** 1434
[21] Guo X M, Wang J, Liu J, Yu H T, Galan R F, Cao Y B and Deng B 2017 *Physica A* **468** 381
[22] Hou J Y, Li X H and Chen J F 2016 *J. Vibroeng.* **18** 4812
[23] Xu B B, Chen D Y, Zhang H and Zhou R 2012 *Nonlinear Dyn.* **81** 1263
[24] Chen D Y, Liu Y X, Ma X Y and Zhang R F 2012 *Nonlinear Dyn.* **67** 893
[25] Zhang H, Chen D Y, Xu B B and Wang F F 2015 *Energy Conv. Manag.* **90** 128
[26] Li H H, Chen D Y, Zhang H, Wu C Z and Wang X Y 2016 *Appl. Energy* **185** 244
[27] Li H H, Chen D Y, Zhang H, Wang F F and Ba D D 2016 *Mech. Syst. Signal Proc.* **80** 414
[28] Li H H, Chen D Y, Zhang X G and Wu Y H 2016 *IET Renew. Power Gen.* **10** 1140
[29] Zeng Y, Zhang L X, Guo Y K, Qian J and Zhang C L 2014 *Nonlinear Dyn.* **76** 1921
[30] Xu B B, Wang F F, Chen D Y and Zhang H 2016 *Energy Conv. Manag.* **108** 478
[31] Pico H N V, Aliprantis D C, McCalley J D, Elia N and Castrillon N J 2015 *IEEE Trans. Power Systems* **23** 632
[32] Salhi I, Doubabi S and Essounbouli N 2010 *Renew. Energy* **35** 2071
[33] Husek P 2014 *Int. J. Electr. Power Energy Syst.* **55** 460
[34] Ding C, Ba D D, Chen D Y and Yuan P 2012 *Engineering Journal of Wuhan University* **45** 187 (in Chinese)
[35] Kishor N, Saini R P and Singh S P 2007 *Renew. Sust. Energ. Rev.* **11** 776
[36] Zhang H, Chen D Y, Wu C Z, Wang X Y, Lee J M and Jung K H 2017 *Energy Conv. Manag.* **138** 375
[37] Shen Z Y 1998 Hydraulic turbine regulation, 3nd edn. (Beijing: Water Power Press) p. 289
[38] Zhang H, Chen D Y, Xu B B, Wu C Z and Wang X Y 2017 *Nonlinear Dyn.* **87** 2519